energies

MDPI

Article

Evaluation of a New Droplet Growth Model for Small Droplets in Condensing Steam Flows

Sima Shabani [1], Mirosław Majkut [1], Sławomir Dykas [1,*], Krystian Smołka [1], Esmail Lakzian [2,3], Mohammad Ghodrati [2] and Guojie Zhang [4]

[1] Department of Power Engineering and Turbomachinery, Silesian University of Technology, 44-100 Gliwice, Poland; sima.shabani@polsl.pl (S.S.); miroslaw.majkut@polsl.pl (M.M.); krystian.smolka@polsl.pl (K.S.)
[2] Center of Computational Energy, Department of Mechanical Engineering, Hakim Sabzevari University, Sabzevar 9617976487, Iran; es.lakzian@pyunji.andong.ac.kr (E.L.); m.qodrati8@gmail.com (M.G.)
[3] Department of Mechanical Engineering, Andong National University, Andong 36729, Republic of Korea
[4] School of Mechanical and Power Engineering, Zhengzhou University, Zhengzhou 450001, China; zhangguojie2018@zzu.edu.cn
* Correspondence: slawomir.dykas@polsl.pl

Abstract: As the condensation phenomenon occurs in the low-pressure stages of steam turbines, an accurate modelling of the condensing flows is very crucial and has a significant impact on the development of highly efficient steam turbines. In order to accurately simulate condensing steam flows, it is essential to choose the right condensation model. Further research to enhance condensation models is of special importance because the outcomes of numerical studies of condensation models in recent years have not been entirely compatible with the experiments and there are still uncertainties in this area. Therefore, the main aim of this paper is to evaluate a proposed droplet growth model for modelling condensation phenomenon in condensing steam flows. The new model is derived to profit from the advantages of models based on the continuum approach for large droplets and those based on the kinetic theorem for small droplets, which results in the model being robust for a wide range of Knudsen numbers. The model is implemented into a commercial CFD tool, ANSYS Fluent 2022 R1, using UDFs. The results of the CFD simulations are validated against experimental data for linear cascades within the rotor and stator blade geometries of low-pressure steam turbine stages. The findings clearly demonstrate the superiority of the new model in capturing droplet growth, particularly for very small droplets immediately following nucleation. In contrast, widely used alternative droplet growth models tend to either underpredict or overpredict the droplet growth rate. This research significantly contributes to the ongoing efforts to enhance condensation modeling, providing a more accurate tool for optimizing the design and operation of low-pressure steam turbines, ultimately leading to a higher energy efficiency and a reduced environmental impact.

Keywords: condensing steam flows; droplet growth model; steam turbine stages; CFD simulations; linear cascades

Citation: Shabani, S.; Majkut, M.; Dykas, S.; Smołka, K.; Lakzian, E.; Ghodrati, M.; Zhang, G. Evaluation of a New Droplet Growth Model for Small Droplets in Condensing Steam Flows. *Energies* **2024**, *17*, 1135. https://doi.org/10.3390/en17051135

Academic Editors: Marco Marengo and Giorgio Ficco

Received: 19 January 2024
Revised: 21 February 2024
Accepted: 24 February 2024
Published: 27 February 2024

1. Introduction

The analysis of the flow through steam turbine blades, aiming to improve the turbines' efficiency, is crucial as steam turbines are used in vast areas of power generation, including nuclear power generation, coal-fired power generation, gas turbine combined-cycle power generation and other power generation systems [1,2]. Nowadays, many researchers and scientists are trying to improve the CFD simulation of steam condensing flows in the low-pressure stages of steam turbines [3–7]. Considering that steam turbines are a vital part of the power industry, it is extremely important to investigate condensing steam flows in the low-pressure stages of a machine. It is also necessary to improve the prediction of the flow behavior and the accuracy of CFD results [8–11].

Condensation occurs in the low-pressure stages of steam turbines, where steam is in the non-equilibrium state, tending to lose its latent heat and turning into liquid droplets. This phenomenon is called homogeneous spontaneous condensation. Two steps are needed to model this condensation phenomenon: modelling of nucleation and modelling of the droplet growth. This study focuses on droplet growth modelling. The gas dynamics theory states that the collision frequency between steam molecules and condensed nuclei is related to the Knudsen number (Kn), which is the ratio of the mean free path of steam molecules to the radii of water droplets. The larger the Knudsen number, the smaller the droplet diameter. Two primary methods for assessing droplet growth are discussed in the literature. First, there is a continuum-based strategy suitable for continuous regimes with low Knudsen numbers (Kn < 0.01). The second strategy is the kinetic-based approach, suitable for free molecular regimes with large Knudsen numbers (Kn > 10). Nevertheless, condensation may also occur in the transition regime (0.01 < Kn < 10). Due to this, it is necessary to establish a relationship that holds in the full range of Knudsen numbers.

Gyarmathy introduced one of the most widely accepted models for droplet growth, utilizing a continuum-based approach. He introduced a correction function for the heat transfer coefficient by utilizing an empirical correlation. Some researchers have used this model in their research [12,13]. Fuchs and Sutugin amended Gyarmathy's equation, proposing the utilization of the mass flow ratio between the transition phase and the free molecular regime as the corrective coefficient. Some researchers used this model in their research [14]. Young [15] introduced a correction factor to Gyarmathy's equation with the aim of enhancing the consistency between the experimental results and theoretical predictions. In order to study condensation on the surface of mercury, Hertz and Knudsen created a model drawing on the kinetic-based method. Some studies used this model in their research [16]. Several models, incorporating simplifications, have been proposed using the Hertz and Knudsen equations. Through an intricate assessment of kinetic models, Puzyrewski and Studzinski [17] examined simplifications related to the droplet radius and the rate of temperature change in condensation flows. Additionally, Puzyrewski and Król [18] created a droplet growth model that resembled Gyarmathy's equation.

While current condensation models remain incomplete, researchers have explored condensing flows through droplet growth models based on both continuum and kinetic approaches. Through the application of semi-empirical correction factors, scientists can fine-tune models to achieve more precise results. Han et al. [19] proposed a coupled model of the heat and mass balance for the droplet growth in wet steam homogeneous condensing flows. Their model corresponds well to the experimental data from Peter and Meyer in the transition region, the Young low-pressure correction model in the free molecular flow region and the Gyarmathy model in the continuous flow region. Sun et al. [20] investigated, numerically, the impact of changing the droplet growth model on the nitrogen condensation flow through de Laval nozzles in ANSYS CFX using the user-defined language. For the condensation model, they used the classical nucleation model with a non-isothermal correction and different droplet growth models including those developed by Gyarmathy and Young. Their findings show that the modification has little impact on the prediction of the condensation onset location but has a significant impact on the development of the droplet size and the relaxation time of gas returning to the state of equilibrium. Zhang et al. [21] suggested a modified model to assess the performance of the steam ejector. To estimate non-equilibrium condensation, they used four models made of different nucleation models and droplet growth models. The findings demonstrate that, compared to the other three models, the modified nucleation model and Young's droplet growth model (ϕ = 0.75, α = 9) show the best potential to predict the pressure distribution and the Wilson point. Zhang et al. [22] provided a modified condensation model to assess the performance of the steam ejector and to optimize the steam ejector design. They predicted the non-equilibrium condensation process in a nozzle and in a steam ejector using four models made up of several nucleation models and droplet growth models. The results showed that the modified condensation model was superior

to the other three models. Wiśniewski et al. [23] evaluated the impact of condensation models on the modelling of condensation phenomena in transonic flows of moist air. They compared the numerical results of the four most popular condensation models with the experimental data for the internal flow through a nozzle and the external flow around an airfoil, and finally recommended the condensation model appropriate for the moist air transonic flow.

To address the requirement for an equation applicable across a broad spectrum of Knudsen numbers, this research proposes a droplet growth model that integrates a continuum-based approach with a correction derived from a kinetic-based model, ensuring adaptability to a wide range of Knudsen numbers. The suggested model is subjected to numerical exploration and executed using the ANSYS Fluent CFD software. The consistent outcomes obtained from the model indicate its suitability for examining steam condensation flows across a diverse spectrum of Knudsen numbers.

2. Physical and Numerical Model

The RANS approach for the compressible steam flow was described in the ANSYS Fluent code in the following way:

$$\frac{\partial}{\partial t}\rho_v + \frac{\partial}{\partial x_j}\rho_v u_j = 0 \tag{1}$$

$$\frac{\partial}{\partial t}\rho_v u_i + \frac{\partial}{\partial x_j}\left(\rho_v u_i u_j + \delta_{ij} p - \tau_{ij}\right) = 0 \tag{2}$$

$$\frac{\partial}{\partial t}\rho_v E_v + \frac{\partial}{\partial x_j}\left(\rho_v E_v u_j + u_j p\right) = \frac{\partial}{\partial x_j}\left(\lambda_v \frac{\partial}{\partial x_j} T_v + \tau_{ij} u_i\right) + S_E \tag{3}$$

where S_E is the source term due to homogeneous condensation:

$$S_E = S_y \cdot L \tag{4}$$

2.1. Condensation Model

To describe the phase change caused by homogeneous condensation, it is important to take into account additional transport equations. The number of droplets per kilogram (n) produced by the nucleation process, and the liquid mass fraction (y) produced by homogeneous condensation, are expressed by the following partial differential equations (PDEs):

$$\frac{\partial \rho_m y}{\partial t} + \frac{\partial}{\partial x_j}\left(\rho_m u_j y\right) = S_y \tag{5}$$

$$\frac{\partial \rho_m n}{\partial t} + \frac{\partial}{\partial x_j}\left(\rho_m u_j n\right) = S_n \tag{6}$$

where S is the source term: in Equation (5) the source is the mass of the liquid condensed due to homogeneous condensation, and in Equation (6) the source is the number of droplets produced per kilogram of steam as a result of the nucleation process. The following formulae define the source terms:

$$S_y = \frac{4}{3}\pi \rho_l r^{*3} J + 4\pi \rho_l n r^2 \frac{dr}{dt} \tag{7}$$

$$S_n = \rho_m J \tag{8}$$

The ANSYS Fluent UDFs were used to introduce these additional transport equations. In Equations (7) and (8), J represents the number of critical radii r^* nuclei that form in 1 m^3

of steam in one second, and ($\frac{dr}{dt}$) represents the droplet growth rate. The nucleation rate is determined based on the classical nucleation theory [24]:

$$J = C\alpha_c \sqrt{\frac{2\sigma}{\pi m_v^3}} \frac{{\rho_v}^2}{\rho_l} \exp\left(-\frac{4\pi\beta_c r^{*2}\sigma}{3k_B T_v}\right) \tag{9}$$

where α_c is the condensation coefficient and in this study, which is considered to be 1. β_c is an empirical correction factor, which is considered to be 1 in this study. C is the non-isothermal correction factor which is proposed by Kantrowitz [25] as follows:

$$C = \left[1 + 2\frac{\gamma_v - 1}{\gamma_v + 1}\frac{L}{RT_v}\left(\frac{L}{RT_v} - \frac{1}{2}\right)\right]^{-1} \tag{10}$$

2.1.1. Continuous Model

The droplet growth phenomenon is always accompanied by the release of latent heat. Due to the small thermal inertia of the droplets, the growth rate can be determined by equating this latent heat release to the energy transferred back to the surrounding vapor, giving:

$$L\frac{dm_l}{dt} = 4\pi r^2 \alpha (T_l - T_v) \tag{11}$$

where α is the heat transfer coefficient between liquid and vapor. Considering a liquid droplet as a sphere, $m_l = \frac{4}{3}\pi r^3 \rho_l$; by substituting this into Equation (11) and simplifying we obtain:

$$\frac{dr}{dt} = \frac{\alpha(T_l - T_v)}{\rho_l L} \tag{12}$$

According to the Clausius–Clapeyron equation [24], the above equation can be written as follows:

$$\frac{dr}{dt} = \alpha \frac{1}{\rho_l}\left(1 - \frac{r^*}{r}\right)\left(\frac{RT_v^2}{L^2}\right) ln(S) \tag{13}$$

Using the Nusselt number (Nu), the heat transfer coefficient can be calculated:

$$Nu = \frac{2r\alpha}{\lambda_v} \tag{14}$$

When assuming a no-slip velocity between the two phases, the Nusselt number transitions to 2.0. This assumption is applicable to condensation flows involving very small droplets ($d < 1$ μ), leading to $\alpha = \frac{\lambda_v}{r}$. Nevertheless, it is essential to integrate a correction function for the heat transfer coefficient within the low-Knudsen number range, $f(Kn)$. Therefore, it can be concluded that $\alpha = \frac{\lambda_v}{r} f(Kn)$. By substituting this into Equation (13):

$$\frac{dr}{dt} = f(Kn)\frac{\lambda_v}{r}\frac{1}{\rho_l}\left(1 - \frac{r^*}{r}\right)\left(\frac{RT_v^2}{L^2}\right) ln(S) \tag{15}$$

As previously stated, Gyarmathy's correction function was the most widely adopted:

$$f(Kn)_{GY} = \frac{1}{1 + 3.18Kn} \tag{16}$$

The evolution of Gyarmathy's model has been discussed by numerous researchers. With the following formulae, Fuch–Sutugin and Young provided the most well-known corrections:

$$f(Kn)_{FS} = \frac{1 + 2.0Kn}{1 + 3.42Kn + 5.32Kn^2} \tag{17}$$

$$f(Kn)_{YO} = \frac{1}{1 + 3.78(1 - \nu)\frac{Kn}{Pr}} \tag{18}$$

The correction factor $(1 - \nu)$ in Equation (18) was considered by Young:

$$\nu = \frac{RT_s}{L}\left(\alpha_{YO} - 0.5 - \left(\frac{2 - q_{YO}}{q_{YO}}\right)\left(\frac{\gamma_v + 1}{\gamma_v}\right)\left(\frac{c_{pv}T_s}{L}\right)\right) \tag{19}$$

where α_{YO} is Young's empirical correction factor set to 9, and q_{YO} is Young's condensation coefficient set to 1 in this study.

2.1.2. Kinetic Model

A rough estimate of the droplet growth can be achieved regardless of droplet size, assuming that there is no significant change in the droplet temperature and the steam and droplet temperatures are the same: $T_l = T_v$, as suggested by Hill [26]. The steam molecules collide into the surfaces of the nuclei; some are caught in the liquid state, while others are reflected. Also, it was assumed that the nuclei's surfaces were flat. The droplet growth equation for the free-molecular regime takes the following form as a result of this assumption, which was added to the model of Hertz and Knudsen, which determines the growth of very small water droplets:

$$\frac{dr}{dt} = \frac{\alpha_c}{\rho_l} \times \frac{p_v - p_s}{\sqrt{2\pi RT}} \tag{20}$$

Using various assumptions, several researchers have developed simpler versions of Equation (20). Puzyrewski and Król proposed the following droplet growth rate equation:

$$\frac{dr}{dt} = \frac{32\alpha_c}{25\pi c_v(2 - \alpha_c)}\frac{\lambda_v}{\rho_l \bar{l}}\left(1 - \frac{r^*}{r}\right)\ln S \tag{21}$$

2.1.3. Proposed Model

As explained in the previous sections, two primary methods for assessing the droplet growth are discussed in the literature. First, there is a continuum-based strategy suitable for continuous regimes with low Knudsen numbers ($Kn < 0.01$). The second strategy is the kinetic-based approach, suitable for free molecular regimes with large Knudsen numbers ($Kn > 10$). The Knudsen number physically determines the ratio of mean free path between steam molecules to the droplet diameter (see Figure 1). According to its definition ($\frac{\bar{l}}{d}$), when the distance between steam molecules is large and the droplet diameter is small, the Kn number will be very large. In this case, the collision frequency between the steam molecules and the droplet is very small. Therefore, the probability of collision between steam molecules and the droplet is reduced, and the droplet growth rate is also reduced. In this case, Kinetic models are used for the droplet growth rate. Conversely, when the distance between steam molecules is small and the droplet diameter is large, the Kn number will be small. In this case, the collision frequency between the steam molecules and the droplet increases and leads to an increase in the probability of condensation and droplet growth. In this case, continuous models are used to calculate the droplet growth rates, as seen in their equations (Equations (16)–(18)), and the Knudsen number plays a significant role in these models.

Nevertheless, condensation may also occur in the transition regime ($0.01 < Kn < 10$). Hence, it becomes crucial to establish a relationship that remains valid across the entire spectrum of Knudsen numbers. Given the model's validity range and the similarities between the equations derived by Gyarmathy and Puzyrewski for continuous and free molecular regimes, combining these models appears reasonable. The Gyarmathy droplet growth equation for the continuum model is obtained by substituting Equation (16) into Equation (15), which is valid for large droplets and wet steam flows. The Puzyrewski droplet growth equation for the kinetic model is in accordance with Equation (21), which is simplified as follows and has acceptable results for small droplets and moist air flows.

Now we are looking for an equation that has good accuracy for wet steam flows and very fine droplets, especially in the initial regions immediately after the nucleation region.

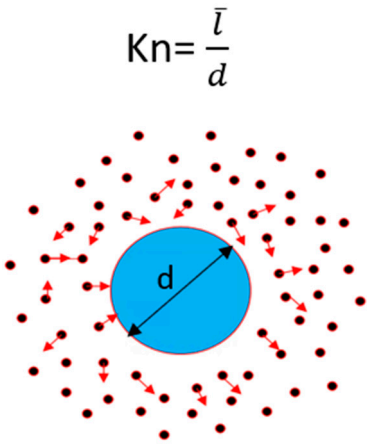

Figure 1. The Knudsen number definition (The blue circle represents the liquid droplet which was surrounded by steam molecules which was shown as black dots. The arrows show the flow path of steam molecules.).

Gyarmathy equation for continuum model

$$\frac{dr}{dt} = \frac{1}{1+3.18Kn}\frac{\lambda_v}{\rho_l r}\left(1-\frac{r^*}{r}\right)\left(\frac{RT_v^2}{L^2}\right)ln(S)$$

Puzyrewski equation for kinetic model

$$\frac{dr}{dt} = \frac{32\alpha_c}{25\pi c_v(2-\alpha_c)}\frac{\lambda_v}{\rho_l \bar{l}}\left(1-\frac{r^*}{r}\right)ln(S) = \frac{1}{\frac{25\pi c_v(2-\alpha_c)}{32\alpha_c}}\frac{\lambda_v}{\rho_l \bar{l}}\left(1-\frac{r^*}{r}\right)ln(S)$$

Equating the right-hand sides of the above two equations and using $Kn = \frac{\bar{l}}{2r}$ and a mathematical simplification, we obtain the following equation.

$$\frac{1}{1+3.18Kn} = \frac{1}{\frac{25\pi c_v(2-\alpha_c)}{16\alpha_c}\left(\frac{RT_v^2}{L^2}\right)Kn}$$

As you can see in the equation above, the empirical coefficient of the continuum model (3.18) can be replaced by the term $\frac{25\pi c_v(2-\alpha_c)}{16\alpha_c}\left(\frac{RT_v^2}{L^2}\right)$ which is based on kinetic models. This idea makes the new equation suitable for high Knudsen numbers, i.e., small droplets, and because this coefficient is multiplied by the Knudsen number, it can also be suitable for large droplets (low Knudsen numbers). Therefore, and also based on the obtained numerical results, the new droplet growth equation, which is as follows, is acceptable for a wide range of Knudsen numbers.

$$\frac{dr}{dt} = \frac{1}{1+\frac{25\pi c_v(2-\alpha_c)}{16\alpha_c}\left(\frac{RT_v^2}{L^2}\right)Kn}\frac{\lambda_v}{\rho_l r}\left(1-\frac{r^*}{r}\right)\left(\frac{RT_v^2}{L^2}\right)ln(S) \quad (22)$$

3. Experimental Test Rig and Boundary Conditions

The experimental data used in this research were obtained from the in-house laboratory [27,28] of Silesian University of Technology. In fact, the examined geometries are placed in the test section of a circuit, which is fed by a 1 MW boiler. The maximum value of the resulting mass flow rate is 3 kg/s. Upstream, a control valve and a desuperheater are installed to provide the desired conditions. The adjustable range for total inlet pressure

inlet total inlet temperature is 70–150 kPa and 70–150 °C. In the test section, there are sensors to measure the static pressure on the surface of the investigated geometries, and we used the measured data to validate the numerical results. The measurement frequency of these sensors is 400 Hz and the measurement duration is 3 s. By averaging between the results obtained from these 1200 samples, the final values were obtained. Figure 2 shows a photo of our in-house test rig.

Figure 2. The SUT test rig.

The investigated geometries are the linear cascades of the rotor and stator blades installed in the test section of a small steam condensing power plant [27,28] located in the Machinery Hall of the Silesian University of Technology. The boundary conditions used for the test cases are shown in Table 1.

Table 1. Boundary conditions for the test cases.

	Stator	**Rotor**
Inlet	P_0 = 103 kPa T_0 = 105.85 °C	P_0 = 65 kPa T_0 = 130.5 °C
Outlet	P_{out} = 42 kPa	P_{out} = 14 kPa

3.1. Linear Stator Blade Cascades

The measuring chamber used for the testing of the steam flow in the stator blade cascade is presented in Figure 3. The geometry of the blades corresponds to that of the last stage stator in the low-pressure part of a real ~200 MW turbine. The test section is made of four blades, which gives three blade-to-blade channels. The cascade basic dimensions are as follows [27]:

- Blade chord in axial direction: 173.97 mm;
- Pitch: 91.74 mm;
- Working medium inflow angle: 0.0°;
- Test section width: 110 mm.

Twenty measuring points for static pressure were positioned on each blade constituting the blade-to-blade channel under examination [27]. Additionally, five pressure (and temperature) measuring points were located at the outlet of the blade cascade, situated 75 mm beyond the trailing edge of the blade. The spacing between these points is 25 mm, as illustrated in Figure 4.

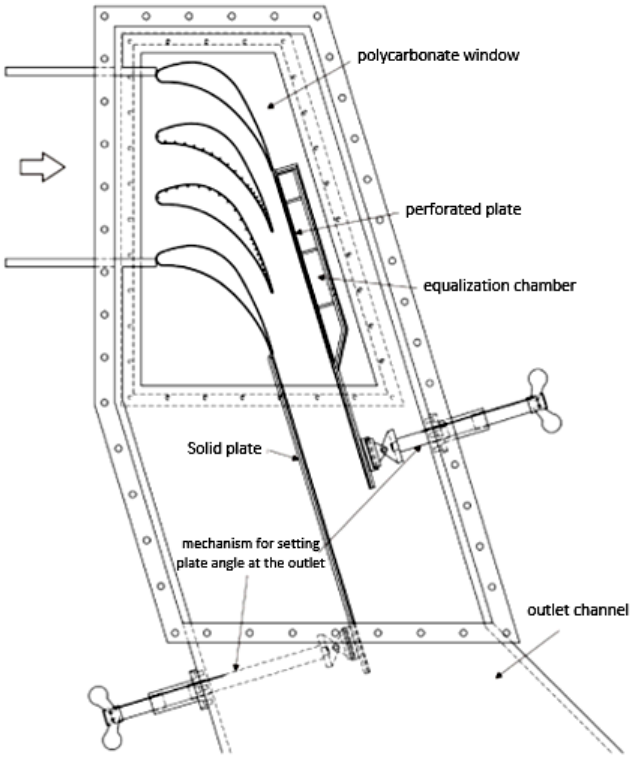

Figure 3. Scheme of a measuring chamber with a linear cascade of stator blades.

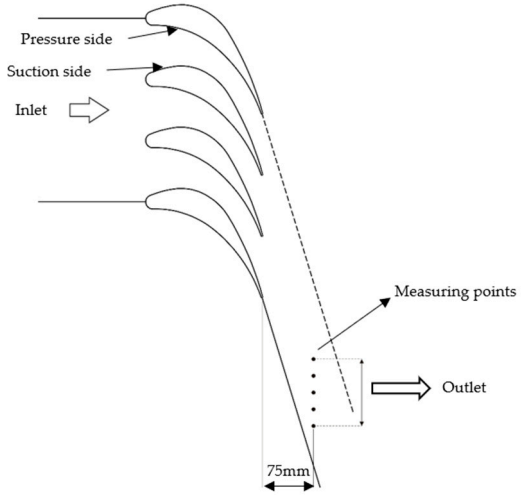

Figure 4. Measuring points at the outlet of test section.

3.2. Linear Rotor Blade Cascades

From the point of view of condensing steam flows, it is equally important to analyze the flow through the rotor blade cascade in the tip cross section of the last (or penultimate) stage of the condensing steam turbine. In the relative system of the tip cross section the transonic flow occurs, in which there is either primary or secondary condensation of water vapor on droplets of the liquid phase already condensed in the stator ring. In state-of-the-art high-power turbines with very high blades in the last stage, supersonic relative velocity can occur in the relative system at the rotor inlet in the tip part, which requires supersonic blade profiles.

Figure 5 shows the measuring chamber with installed rotor blades with a profile that matches the tip geometry of the 200 MW turbine. In order to fit the blade cascade into the measuring chamber and to create the possibility of measuring static pressure on the blade surface, the profile was enlarged from the initial size by 2.5 times.

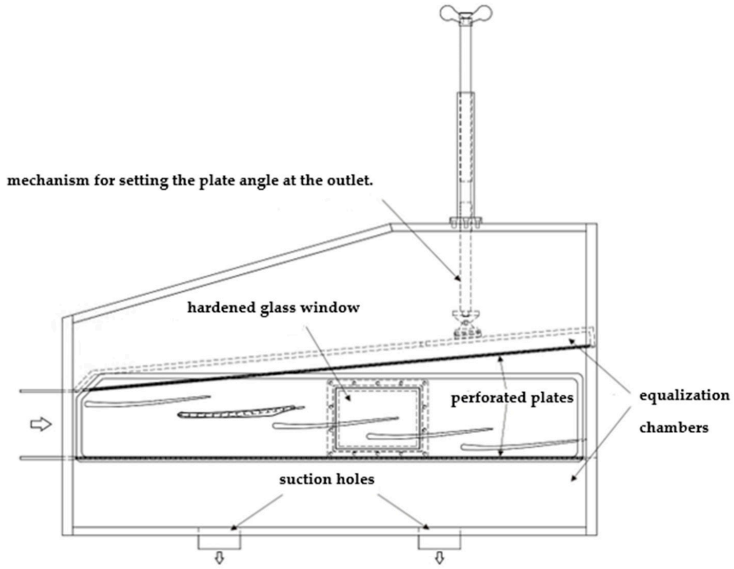

Figure 5. Diagram of the measuring chamber with a linear cascade of rotor blades.

The cascade includes five blades which create four blade-to-blade channels. Owing to the use of an adjustable porous plate restricting the cascade outlet channel (the so-called tailboard) (Figure 5), a high periodicity is maintained for all blade channels in the cascade. This was confirmed by CFD simulations for the entire cascade and by static pressure measurements upstream and downstream of the cascade. The cascade basic dimensions are as follows [28]:

- Blade chord in axial direction: 240.17 mm;
- Pitch: 180 mm;
- Working medium inflow angle: 0.0°;
- Test section width: 110 mm.

Fifteen measuring points for static pressure were positioned on each blade constituting the blade-to-blade channel under examination [28].

4. Results and Discussion

The main purpose of this study was using the proposed correction equation for droplet growth calculations in condensing steam flows and comparing the results with the most popular droplet growth models, such as the Gyarmathy (GY), the Fuchs–Sutugin (FS) and the Young (YO) model. Numerical modeling has been carried out in ANSYS Fluent using User Defined Functions (UDFs). The governing equations including the RANS equations (mass and momentum and energy conservation equations) were applied for a steady state 2D compressible flow. Two additional equations (Transport equations) have been used to predict the liquid phase quantity. The K-ω SST turbulence model has been employed to consider the turbulence flow effects. For estimating liquid and vapor thermodynamic properties, NIST real gas models were used, which employ a shared library to estimate various fluids properties. The various droplet growth models were applied through compiling UDFs into the ANSYS Fluent. The technique of a pressure-based approach was employed, and the coupling of pressure and velocity was ensured through the high-quality Rhie–Chow scheme. The spatial discretization of pressure and momentum was carried out using the upwind second-order scheme. On the other hand, the MUSCL third-order discretization was utilized for density, turbulent kinetic energy, energy and the dissipation rate. Furthermore, for the wet steam parameters, the second-order upwind discretization was applied. The convergence criterion for all parameters involved in the equations is supposed to be 10^{-6}. It is assumed that the volume occupied by droplets in the two-phase non-equilibrium flow can be negligible in some simplifications in comparison to the vapor volume. The model does not account for the interaction between droplets, so it leads to ignoring some phenomenon like coalescence and breakage within the droplets. The

two-phase flow model assumed a no-slip flow. As the velocity difference between the two phases is small and negligible, the droplet–steam relative velocity is omitted, i.e., a droplet moves at the same velocity as water vapor. This assumption considered the velocity of the two phases to be equal, so it simplifies our flow-governing equations.

According to Figures 6 and 7, for result validation, the numerical results of the static pressure distribution across the stator and rotor blades are compared with experimental data. Furthermore, the results obtained by the new droplet growth model (red line) are compared with those obtained by the other droplet growth models (black line). In the presented cases, the results obtained by the GY, FS and YO models coincide. Therefore, they appear as a single line in the figures. For the proposed model, we evaluated the effect of different values of α_c (condensation coefficient) on the results, and we found that for the stator case $\alpha_c = 0.02$ and for the rotor case $\alpha_c = 0.05$, which matched the experimental data. For this reason, we only present the results for these values. As can be seen in Figures 6 and 7, the new model predicts the condensation shock wave location and intensity more accurately than the other models. The GY, FS and YO models give acceptable results for large droplets (low Knudsen numbers) in the continuous region. However, the new model calibrates the droplet growth for very small droplets (large Knudsen numbers), i.e., just after nucleation. It is thus better than the other models, which tend to underpredict the droplet growth rate. It can be concluded that the new model is applicable for a broad range of Knudsen numbers.

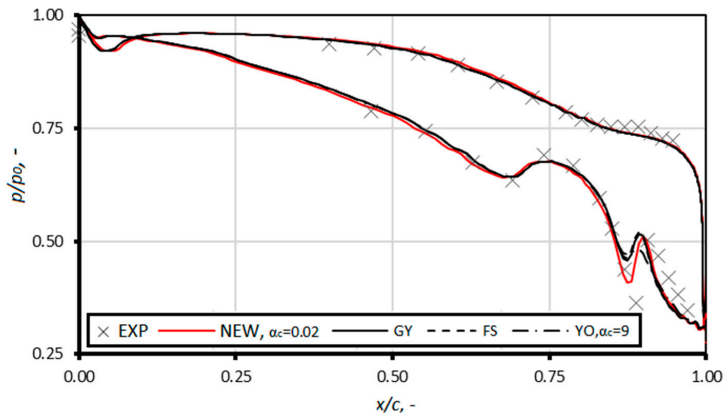

Figure 6. Static pressure distribution on the stator blade surface for different models.

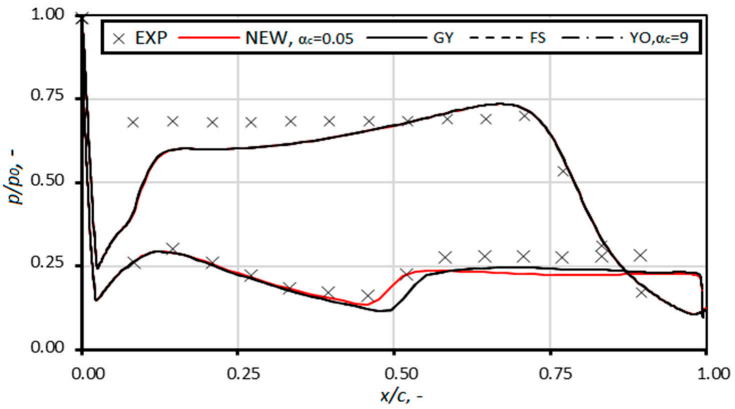

Figure 7. Static pressure distribution on the rotor blade surface for different models.

Figures 8 and 9 present the Mach number and wetness fraction distribution contours throughout the stator blade cascade for all the droplet growth models. As can be seen, there is no significant difference in Mach number contours for different cases, but in wetness contours, the Yong model shows lower values of wetness than the other models.

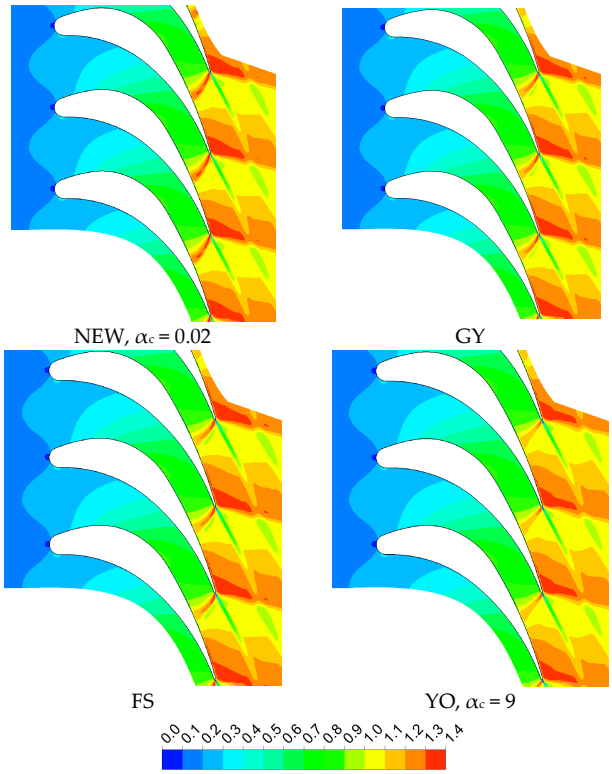

Figure 8. Mach number distribution throughout the stator blade cascade.

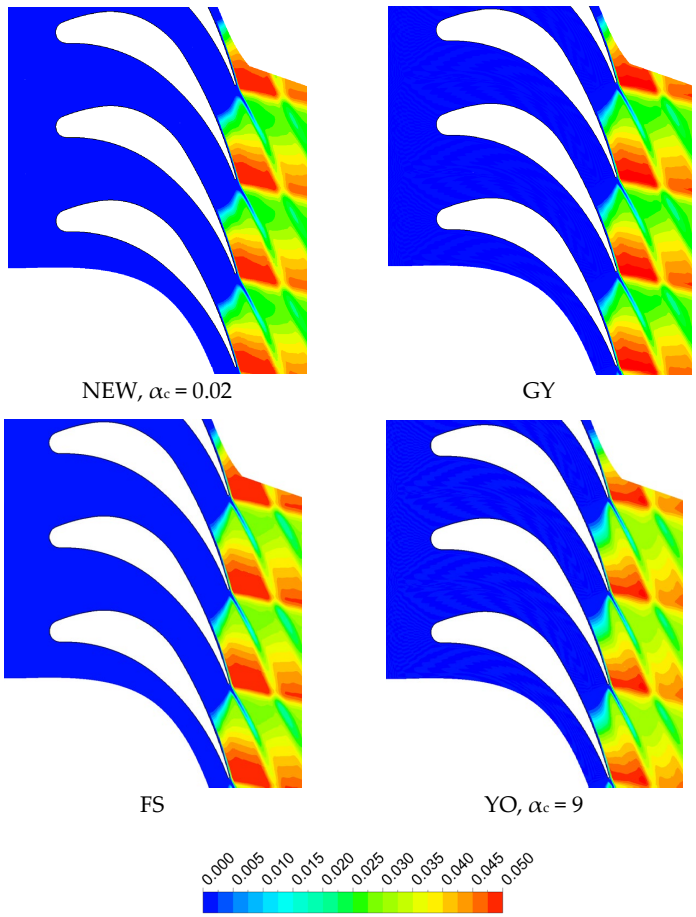

Figure 9. Wetness fraction distribution throughout the stator blade cascade.

Figures 10 and 11 present the Mach number and wetness fraction distribution contours through a rotor blade cascade for all the droplet growth models. As can be seen, the Mach number values for the Yong model are lower than the others. The wetness fraction values for the Yong model are the highest, and the liquid phase appears earlier in this model than the others. The Gyarmathy and Fuchs–Sutugin models show the lowest values of wetness.

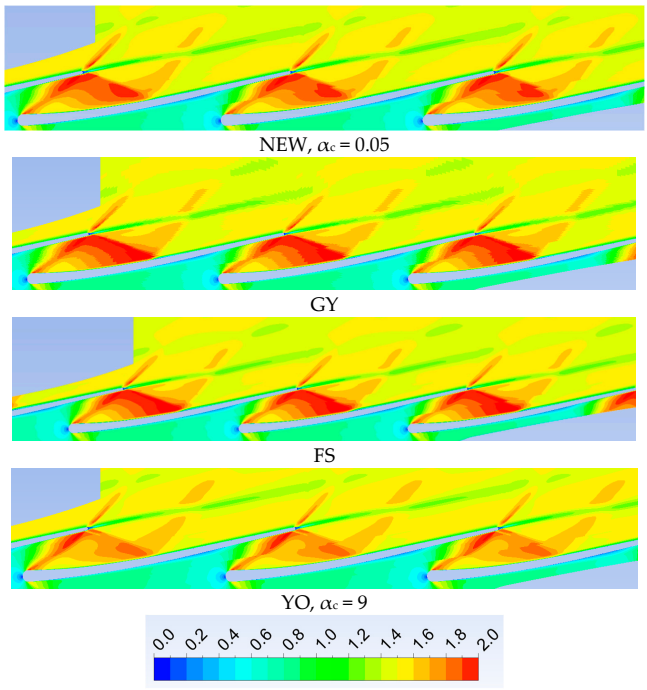

Figure 10. Mach number distribution throughout the rotor blade cascade.

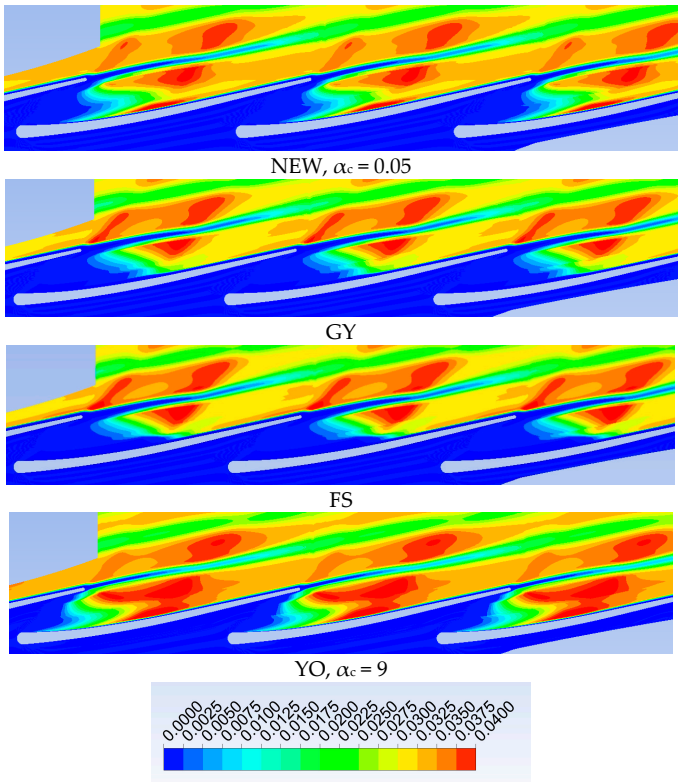

Figure 11. Wetness fraction distribution throughout the rotor blade cascade.

5. Conclusions

This study investigates the steam condensing flow through stator and rotor blade cascades corresponding to stages of the low-pressure steam turbine. The main aim of this study was to propose a new droplet growth model which gives acceptable results in a broad range of Knudsen numbers. A droplet growth model is suggested based on a continuum-based model combined with a large Knudsen number correction based on kinetic-based model. The proposed model was numerically implemented using the ANSYS Fluent CFD program and compared with the most popular droplet growth models. For validation purposes, the numerical results of the static pressure distribution across the blade surface for different models are compared with experimental data.

Comparing the results obtained from different models, it can be stated that the new model demonstrates the best agreement with the experimental data and predicts the condensation wave location and intensity more accurately than the others. The reliable results produced by the model suggest that it can be used to investigate steam condensing flows in a broad range of Knudsen numbers. The research results also indicate that, due to the complexity of phase-change phenomena, it is not enough to simply choose a droplet growth model based on the literature. Further studies are needed to obtain a deeper insight into the occurring phenomena. Moreover, as confirmed by the results, the condensation phenomenon has a significant influence on the pressure distribution due to the appearance of the condensation wave. It affects the Mach number distribution in the blade-to-blade channel and, in turn, the expansion efficiency and the blade working conditions. This highlights the necessity for more study into phase-change multiphase flows to develop reliable condensation models applicable in the design and use of high-efficient turbomachines.

Author Contributions: Conceptualization, S.S.; methodology, M.M. and S.D.; software, S.S.; validation, S.S.; formal analysis, S.S.; investigation, S.S.; resources, M.M., K.S. and S.D.; data curation, S.S.; writing—original draft preparation, S.S.; writing—review and editing, S.S., M.M., S.D., E.L., M.G. and G.Z.; visualization, S.S.; supervision, M.M., S.D. and E.L.; project administration, M.M. and S.D. All authors have read and agreed to the published version of the manuscript.

Funding: This research was funded by the National Science Centre of Poland under grant number 2020/37/B/ST8/02369 and by statutory research funds for young scientists.

Data Availability Statement: The data that support the findings of this study are available from the corresponding author upon reasonable request.

Conflicts of Interest: The authors declare no conflicts of interest.

Nomenclature

c_v	Specific heat in constant volume, J kg^{-1}K^{-1}
c_p	Specific heat in constant pressure, J kg^{-1}K^{-1}
E	Total internal energy, J kg^{-1}
J	Nucleation rate, m^{-3}s^{-1}
k_B	Boltzmann constant, J K^{-1}
Kn	Knudsen number, $\frac{\bar{l}}{2r}$
$\bar{l}$	Mean free path
L	Latent heat, J kg^{-1}
m	Molecular mass, kg
n	Number of droplets, m^{-3}
Nu	Nusselt number
p	Pressure, pa
Pr	Prandtl number
r	Droplet radius, m
r^*	Critical droplet radius, m
R	Gas constant, J kg^{-1}K^{-1}
S	Supersaturation ratio, $\frac{p}{p_s(T_v)}$

T	Temperature, K
t	Time, s
u	Velocity vector, m s^{-1}
x	Axial coordinate, m
y	Wetness fraction
Greek symbols	
α	Heat transfer coefficient
α_c	Condensation coefficient
γ	Ratio of specific heat
δ	Kronecker delta
λ	Thermal conductivity, W $m^{-1}K^{-1}$
ρ	Density, kg m^{-3}
σ	Surface tension, N m^{-1}
τ	Stress tensor, Pa
Subscripts	
l	Liquid
s	Saturation
v	Vapor

References

1. Yousefi Rad, E.; Mahpeykar, M.R. A Novel Hybrid Approach for Numerical Modeling of the Nucleating Flow in Laval Nozzle and Transonic Steam Turbine Blades. *Energies* **2017**, *10*, 1285. [CrossRef]
2. Fan, S.; Wang, Y.; Yao, K.; Shi, J.; Han, J.; Wan, J. Distribution Characteristics of High Wetness Loss Area in the Last Two Stages of Steam Turbine under Varying Conditions. *Energies* **2022**, *15*, 2527. [CrossRef]
3. Lakzian, E.; Ramezani, M.; Shabani, S.; Salmani, F.; Majkut, M.; Kim, H.D. The search for an appropriate condensation model to simulate wet steam transonic flows. *Int. J. Numer. Methods Heat Fluid Flow* **2023**, *33*, 2853–2876. [CrossRef]
4. Halama, J.; Fořt, J. Numerical simulation of transonic flow of wet steam in nozzles and turbines. *Computing* **2013**, *95*, 303–318. [CrossRef]
5. Ihm, S.W.; Kim, C. Computations of homogeneous equilibrium two-phase flows with accurate and efficient shock-stable schemes. *AIAA* **2008**, *46*, 3012–3037. [CrossRef]
6. Grübel, M.; Starzmann, J.; Schatz, M.; Eberle, T.; Vogt, D.M.; Sieverding, F. Two-phase flow modeling and measurements in low-pressure turbines: Part 1—Numerical validation of wet steam models and turbine modeling. *Trans. ASME J. Eng. Gas Turbines Power* **2015**, *137*, 042602. [CrossRef]
7. Yamamoto, S.; Daiguji, H. Higher-order-accurate upwind schemes for solving the compressible Euler and Navier-stokes equations. *Comput. Fluids* **1993**, *22*, 259–270. [CrossRef]
8. Mirafiori, M.; Tancon, M.; Bortolin, S.; Del Col, D. Modeling of growth and dynamics of droplets during dropwise condensation of steam. *Int. J. Heat Mass Transf.* **2024**, *222*, 125109. [CrossRef]
9. Sidin, R.S.R.; Hagmeijer, R.; Sachs, U. Evaluation of master equations for the droplet size distribution in condensing flow. *Phys. Fluids* **2009**, *21*, 073303. [CrossRef]
10. Shabani, S.; Majkut, M.; Dykas, S.; Smołka, K.; Lakzian, E.; Zhang, G. Validation of the CFD Tools against In-House Experiments for Predicting Condensing Steam Flows in Nozzles. *Energies* **2023**, *16*, 4690. [CrossRef]
11. Guo, Y.; Wang, R.; Zhao, D.; Gong, L.; Shen, S. Numerical Simulation of Vapor Dropwise Condensation Process and Droplet Growth Mode. *Energies* **2023**, *16*, 2442. [CrossRef]
12. Peeters, P.; Luijten, C.C.M.; van Dongen, M.E.H. Transitional droplet growth and diffusion coefficients. *Int. J. Heat Mass Transf.* **2001**, *44*, 181–193. [CrossRef]
13. Shabani, S.; Majkut, M.; Dykas, S.; Wiśniewski, P.; Smołka, K.; Cai, X.; Zhang, G. Numerical analysis of the condensing steam flow by means of ANSYS Fluent and in-house academic codes with respect to the capacity for thermodynamic assessment. *Front. Energy Res.* **2022**, *10*, 902629. [CrossRef]
14. Ezhova, E.; Kerminen, V.; Lehtinen, K.; Kulmala, M. A simple model for the time evolution of the condensation sink in the atmosphere for intermediate Knudsen numbers. *Atmos. Chem. Phys.* **2018**, *18*, 2431–2442. [CrossRef]
15. Chandler, K.D.; White, A.J.; Young, J.B. Non-equilibrium wet-steam calculations of unsteady low-pressure turbine flows. *Proc. IMechE Part A J. Power Energy* **2014**, *228*, 143–152. [CrossRef]
16. Pathak, H.; Mullick, K.; Tanimura, S.; Wyslouzil, B. Nonisothermal Droplet Growth in the Free Molecular Regime. *Aerosol Sci. Technol.* **2013**, *47*, 1310–1324. [CrossRef]
17. Puzyrewski, R.; Studzinski, W. One-dimensional water vapor expansion with condensation at higher pressures. *Int. J. Multiph. Flow* **1980**, *6*, 425–439. [CrossRef]
18. Puzyrewski, R.; Król, T. Numerical analysis of Hertz-Knudsen model of condensation upon small droplets in water vapor. *IFFM* **1976**, *70*, 285–307.

19. Han, X.; Han, Z.; Zeng, W.; Quan, J.; Wang, Z. Coupled Model of Heat and Mass Balance for Droplet Growth in Wet Steam Non-Equilibrium Homogeneous Condensation Flow. *Energies* **2017**, *10*, 2033. [CrossRef]
20. Sun, W.; Chen, S.; Hou, Y.; Bu, S.; Ma, Z.; Zhang, L. Numerical Studies of Nitrogen Spontaneous Condensation Flow in Laval Nozzles using Varying Droplet Growth Models. *Int. J. Multiph. Flow* **2019**, *121*, 103118. [CrossRef]
21. Zhang, G.; Zhang, X.; Wang, D.; Jin, Z.; Qin, X. Performance evaluation and operation optimization of the steam ejector based on modified model. *Appl. Therm. Eng.* **2019**, *163*, 114388. [CrossRef]
22. Zhang, G.; Dykas, S.; Yang, S.; Zhang, X.; Li, H.; Wang, J. Optimization of the primary nozzle based on a modified condensation model in a steam ejector. *Appl. Therm. Eng.* **2020**, *171*, 115090. [CrossRef]
23. Wiśniewski, P.; Majkut, M.; Dykas, S.; Smołka, K.; Zhang, G.; Pritz, B. Selection of a steam condensation model for atmospheric air transonic flow prediction. *Appl. Therm. Eng.* **2022**, *203*, 117922. [CrossRef]
24. Bakhtar, F.; Young, J.B.; White, A.J.; Simpson, D.A. Classical Nucleation Theory and Its Application to Condensing Steam Flow Calculations. *Proc. Inst. Mech. Eng. Part C J. Mech. Eng. Sci.* **2005**, *219*, 1315–1333. [CrossRef]
25. Shabani, S.; Majkut, M.; Dykas, S.; Smołka, K.; Lakzian, E. An investigation comparing various numerical approaches for simulating the behaviour of condensing flows in steam nozzles and turbine cascades. *Eng. Anal. Bound. Elem.* **2024**, *158*, 364–374. [CrossRef]
26. Hill, P.G. Condensation of water vapour during supersonic expansion in nozzle. *J. Fluid Mech.* **1966**, *25*, 593–620. [CrossRef]
27. Dykas, S.; Majkut, M.; Strozik, M.; Smołka, K. Losses Estimation in Transonic Wet Steam Flow through Linear Blade Cascade. *J. Therm. Sci.* **2015**, *24*, 109–116. [CrossRef]
28. Dykas, S.; Majkut, M.; Smołka, K.; Strozik, M. Study of the wet steam flow in the blade tip rotor linear blade cascade. *Int. J. Heat Mass Transf.* **2018**, *120*, 9–17. [CrossRef]